Final Draft
of the original manuscript:

Busch, N.; Jepsen, J.; Pistidda, C.; Puszkiel, J.A.; Karimi, F.; Milanese, C.;
Tolkiehn, M.; Chaudhary, A.-L.; Klassen, T.; Dornheim, M.:
**Influence of milling parameters on the sorption properties of the
LiH-MgB2 system doped with TiCl3**

Influence of milling parameters on the sorption properties of the LiH-MgB$_2$ system doped with TiCl$_3$

Nina Busch[a], Julian Jepsen[a], Claudio Pistidda[a], Julián A. Puszkiel[a,b], Fahim Karimi[a], Chiara Milanese[c], Martin Tolkiehn[d], Anna-Lisa Chaudhary[a]*, Thomas Klassen[a], Martin Dornheim[a]

[a] Institute of Materials Research, Helmholtz-Zentrum Geesthacht, Max-Planck-Straße 1, D-21502 Geesthacht , Germany.

[b] Consejo Nacional de Investigaciones Científicas y Técnicas (CONICET), Combatientes de Malvinas 3150, 1427, Buenos Aires, Argentina.

[c] Pavia H$_2$ Lab, Department of Chemistry, Physical Chemistry Division, University of Pavia, Viale Taramelli 16, I-27100 Pavia, Italy.

[d] SRXPD beamline HASYLAB, (Deutsches-Elektronen-Synchrotron DESY), Notkestrasse 85, D-22607 Hamburg, Germany.

* Corresponding author: Anna-Lisa Chaudhary Tel.: +49 4152 87 2647; fax: +49 4152 87 2625. E-mail address: anna-lisa.chaudhary@hzg.de.

Abstract

Hydrogen sorption properties of the LiH-MgB$_2$ system doped with TiCl$_3$ were investigated with respect to milling conditions (milling times, ball to powder (BTP) ratios, rotation velocities and degrees of filling) to form the reactive hydride composite (RHC) LiBH$_4$-MgH$_2$. A heuristic model was applied to approximate the energy transfer from the mill to the powders. These results were linked to experimentally obtained quantities such as crystallite size, specific surface area (SSA) and homogeneity of the samples, using X-ray diffraction (XRD), the Brunauer-Emmett-Teller (BET) method and scanning electron microscopy (SEM), respectively. The results show that not only the crystallite size and SSA were crucial for the sorption kinetics but also the homogeneous dispersion of the reactants plays a significant role.

Keywords

Hydrogen storage; Reactive Hydride Composites; LiBH$_4$; MgH$_2$; ball-milling; sorption

Introduction

Hydrogen can be produced and used as an energy carrier with significantly reduced carbon emissions compared to current fossil fuel driven technologies. The concept of a hydrogen economy is based on the production of hydrogen from renewable energy sources and then

used in combination with a fuel cell to produce energy for a range of applications [1]. An effective hydrogen system requires a suitable method of hydrogen storage to allow for continuous clean energy supply. One such storage solution is the use of metal hydrides. Metal hydrides are able to store and release hydrogen by forming and breaking chemical bonds. The main advantage of metal hydride storage is the higher volumetric density of hydrogen compared to compressed or liquid hydrogen. Complex hydrides are, especially, very promising as hydrogen-storage materials, due to their high gravimetric and volumetric capacities [2]. In particular, $LiBH_4$ possesses the highest hydrogen capacity (18 wt%) [3]. However, its reversibility is limited, due to formation of stable decomposition products [4].

Reversibility of $LiBH_4$ at moderate conditions was achieved by using the RHCs approach [5], where a metal hydride is added to $LiBH_4$. This approach leads to themodynamic destabilisation of the mixture during desorption [6-9]. The $LiBH_4$-MgH_2 composite system (reaction equation 1) has an especially high volumetric density with a reversible hydrogen capacity of c.a. 11 wt% and improved economic advantages [10]. However, the disadvantage of this system is its sluggish sorption kinetics.

$$2\,LiH + MgB_2 + 4H_2 \leftrightarrow 2\,LiBH_4 + MgH_2 \qquad (1)$$

Tailoring ball milling conditions prior to hydrogenation and dehydrogenation processes is a proven method of improving reaction kinetics [7, 9, 11]. For synthesis and modification of nano-sized structures, high-energy ball milling is a well-established method [12-15]. Another alternative is to add transition metal halides to increase significantly the sorption kinetics. The impact of transition metal halides has been studied extensively [16-19]. Their addition to the system reduces particle and crystallite size of the powders, and increases the number of lattice defects and grain boundaries. This in turn leads to improvement of the sorption kinetics of hydrogen due to higher surface area and increased diffusion paths along the phase and crystallite boundaries. Thus, to address kinetic issues of this system, the composite system LiH-MgB_2 was milled with $xTiCl_3$ (x =0.05, 0.025) as an additive using a planetary ball mill whilst systematically varying the operating conditions. A heuristic model can be used to estimate the energy transfer from the milling process [20, 21], including the operating parameters of the mill as well as the interaction with the powders inside the milling vial with the balls. Once calculated, the effect of energy transfer can be discussed within the context of material properties and the consequent relationship to reaction kinetic behaviour. Therefore, conclusions can be drawn on the optimisation of ball milling conditions for the LiH-MgB_2 system with $TiCl_3$ in order to improve the overall sorption behaviour.

Experimental

All materials were handled in a continuously purified argon atmosphere glove box (MBraun, Germany) (O_2 < 10 ppm, H_2O < 10 ppm). LiH (Alfa Aesar , 99.4 %), MgB_2 (Alfa Aesar, 96.7 %), and $TiCl_3$ (Sigma Aldrich, 99.995 %) were milled together in the stoichiometric ratio 2 LiH + MgB_2 + $xTiCl_3$ where x = 0.025 or x = 0.05. A planetary ball mill Pulverisette-5 (Fritsch, Germany) was used in an argon atmosphere glove box with tempered steel (1.3505) milling vials (335 mL) and 10 mm diameter balls. Milling conditions were systematically varied and are listed in Table 1. Unmilled samples of both stoichiometries were hand shaken in a closed glass vial for one minute to compare with the milled samples.

Table 1: Milling parameters systematically adjusted for the 2 LiH + MgB_2 + $xTiCl_3$ (where x = 0.025 or x = 0.05) reactants. [*] refers to the planetary ground plate. [**] refers to the volume fraction of the milling balls in the vial.

Ball to Powder Ratio	Mill Rotational Velocity[*] (rpm)	Degree of Filling[**] (%)	Milling Time (h)	
5:1	50	10	2	10
10:1	130	25	4	15
20:1	230	50	6	20
40:1	330	75	8	30

The model used to approximate the energy-transfer can be found in Burgio et al. [20]. The total energy transferred from the mill and milling balls, P*, can be approximated as a function of yield coefficient, (φ_b, related to the degree of filling or the volume fraction of milling balls in the vial), number (N_b), diameter (d_b) and mass (m_b) of balls, total milling time (t), angular velocity of the plate (Ω_p), angular velocity of the vial (ω_v), distance of the vial to its periphery (r_v), distance from the centre of the mill to the centre of the vial (R_p) and the total powder weight (*PW*) (equation 2). This publication [20] uses a cubic arrangement of the milling balls at rest whereas this study modifies this for a hexagonal arrangement due to its lower volume vacancy.

$$P* = -\varphi_b \cdot N_b \cdot m_b \cdot t \cdot \left(\Omega_p - \omega_v\right) \left[\frac{\omega_v^3 \cdot \left(r_v - \frac{d_b}{2}\right)}{\Omega_p} + \Omega_p \cdot \omega_v \cdot R_p \right] \cdot \frac{\left(r_v - \frac{d_b}{2}\right)}{2 \cdot \pi \cdot PW}$$

(2)

Sorption properties were measured with a Sievert apparatus (HERA Hydrogen Systems, Canada) with 50 bar H_2 at 350 °C for absorption and 3 bar H_2 at 400 °C for desorption. All samples milled for 2, 10 and 30 hours were cycled twice. X-Ray Diffraction (XRD) measurements were performed in transmission mode at the Beamline D3 of the Hasylab in

DESY (Hamburg, Germany) using a MarCCD-165 area detector and a wavelength of 0.499 Å. Crystallite size was calculated using Rietveld refinement with MAUD software (Materials Analysis Using Diffraction, Italy). Specific surface area (SSA) was determined with the Brunauer-Emmet-Teller (BET) method using the ASAP 2020 physisorption analyser (Micromeritics, Norcross, USA) after being pre-treated at 100 °C under vacuum for 20 hours.

Morphology and phase identification was obtained using a Scanning Electron Microscope (SEM, Zeiss, Germany), equipped with a backscattered electron (BSE) detector and an Energy-Dispersive X-Ray Spectrometer (EDS).

Results and Discussion

The relationship between the energy transfer (equation 2) from the milling process to the powders under the conditions listed in Table 1 and sorption times are shown in Figure 1. The absorption and desorption times were taken when 75 % of the maximum hydrogen capacity was reached.
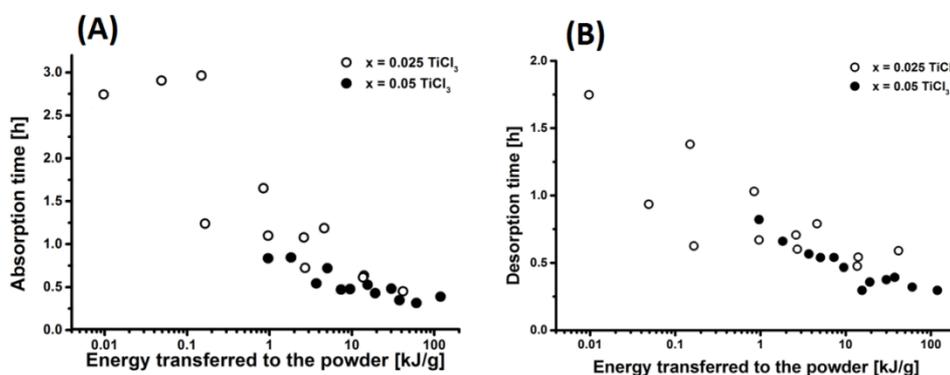
Figure 1: (A) Absorption and (B) desorption times shown as a function of the calculated energy transferred to the powder during the milling process.

From Figure 1, it can be seen that for both reactions, an increase in energy transfer results in a decrease in reaction time. This is a direct reflection of the model (equation 2) that shows longer milling time, faster rotation velocities and larger BTP ratios result in higher energy-transfers. It is also evident that higher additive concentration leads to improved sorption times. This could be due to the additive providing nucleation sites for boron containing compounds or to more effective grain refinement [17, 22-24]. Additionally, with this increase in energy transfer there is a narrowing of reaction time distribution. A tendency toward a plateau in sorption times is visible such that any increase in energy transfer will have no further effect. This too could be attributed to the grain refinement effect of the additive [16,

4

17]. To separate the effect of additive vs. milling conditions, each concentration was kept constant, and comparisons are made with changes in milling conditions.

The energy transfer model, shown in equation 2, shows that larger BTP ratios and longer milling times will linearly increase the total transferred energy to the powder. To show this experimentally, crystallite size and specific surface area were determined after milling, and the relationship with energy transfer determined (Figure 2). Figure 2a gives the crystallite size of the main reactant, MgB_2 with respect to energy transfer and 2b shows the resultant relationship with reaction kinetics. A clear trend can be observed with all variations in BTP ratio, where an increase in energy transfer results in a decrease in crystallite size of MgB_2 (Figure 2a) until a plateau is reached around 5 nm. This plateau occurs at approximately 20 $kJ.g^{-1}$ of energy transfer. As expected, with smaller crystallite size, the reaction kinetics improve resulting in less time for both absorption and desorption (Figure 2c) and these results correlate well with the data shown in Figure 1 relating energy transfer to reaction times.
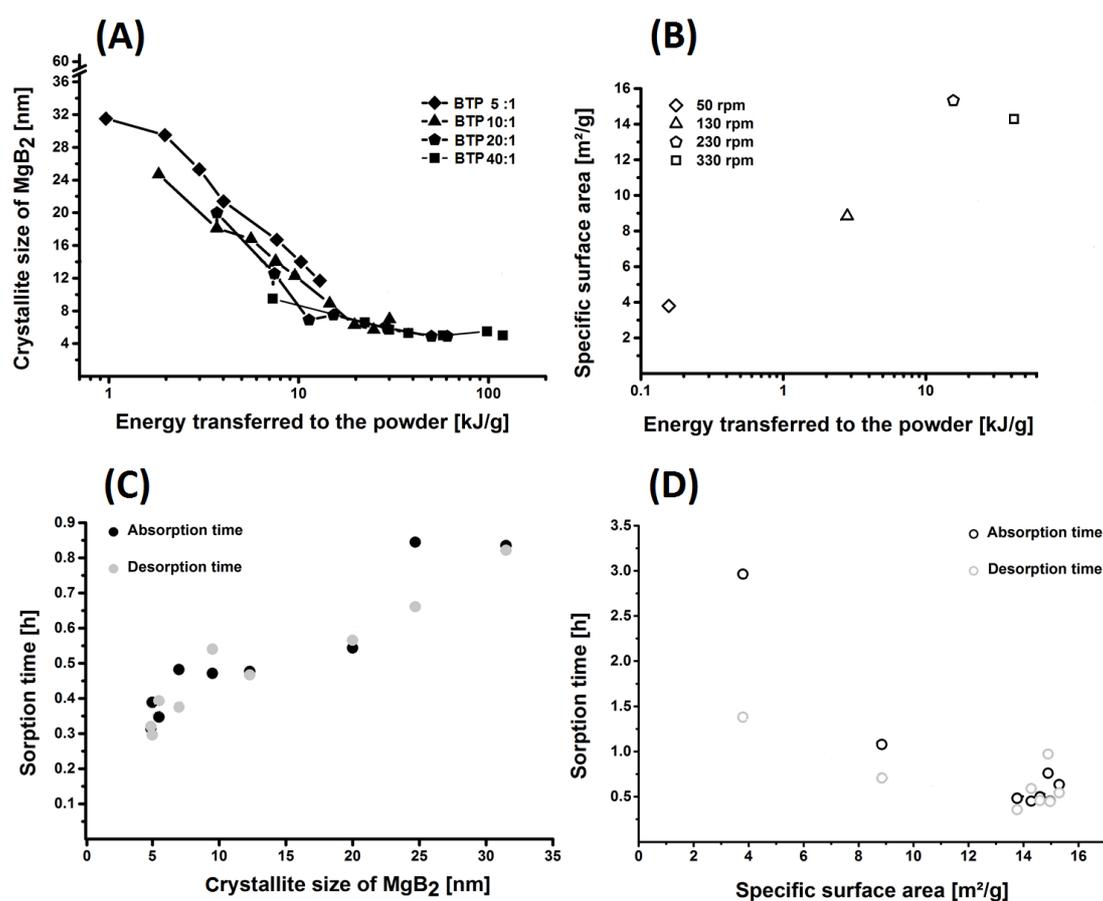
Figure 2: (A) Crystallite size of MgB_2 and (B) specific surface area as a function of the energy transferred to the powder. Sorption times changes with (C) crystallite size of MgB_2 and (D) specific surface area.

Specific surface area was also measured and plotted against energy transfer (Figure 2b) and sorption times (Figure 2d). The initial SSA before milling was less than 4 $m^2.g^{-1}$ and it appears that a maximum SSA (15 $m^2.g^{-1}$) is reached at 230 rpm for an energy transfer of 20 $kJ.g^{-1}$. Any increase in energy transfer did not increase the SSA after this point (20 $kJ.g^{-1}$). With a reduction in crystallite size it is assumed that particle size will also decrease, therefore, the increase in SSA will also plateau with respect to energy transfer. This becomes more evident when sorption times are plotted against SSA (Figure 2d). Here, sorption times decrease with an increase in SSA until the limit is reached.

Interestingly, the degree of filling had a different effect on sorption time compared to the previously mentioned parameters. Figure 3 shows sorption times with respect to degree of filling. According to equation 2, there is a linear relationship between degree of filling and energy transfer (yield coefficient). This is true for a low degree of filling, when there are fewer milling balls present; the energy transfer to the powder is low as there are less opportunities for the powder and milling media to interact. However, this model is not able to take into account the fixed volume of the milling vial. Therefore, at higher degrees of filling, the model predicts higher energy transfer, however, when the vial is full, the balls are blocking each other and consequently there is less movement of the balls, thus reducing their impact on the powder. As shown in Figure 3, for both absorption and desorption, a maximum or optimum value of energy transfer is reached resulting in a minimum sorption time. These experiments have shown that an optimum of 50 % filled gives the maximum amount of energy transfer with shortest sorption times.
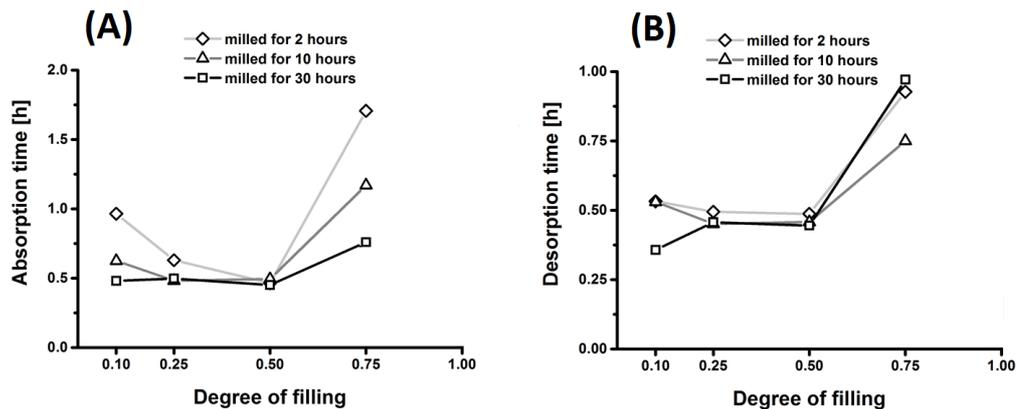
Figure 3: (A) Absorption and (B) desorption time with respect to energy transferred from the milling process to the powder.

Homogeneity of additive plays an important role in sorption behaviour [25, 26] and was therefore observed using SEM on the LiH-MgB$_2$ system with TiCl$_3$ additive before and after milling. A full range of SEM analyses was done on all the samples, however, only two

extreme cases are shown here, i.e. the unmilled sample and the 30 h milled sample (Figure 4). The light elements H, Li and B have physical detection limitations including low fluorescence yield, and peak overlaps with heavier elements, and it was assumed that any B present was bound to the Mg and that the compound LiH appears as the darker particles.
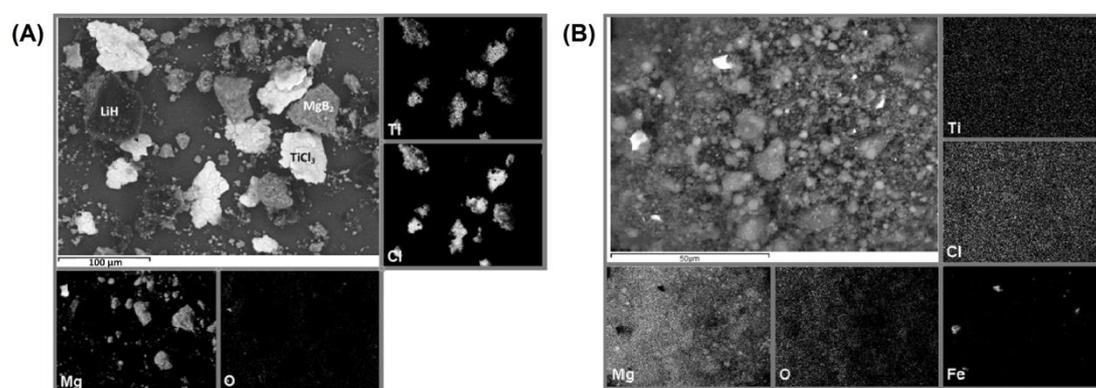
Figure 4: SEM images in backscattering and EDS modes (A) unmilled sample (B) and a 30 h milled sample, with elemental distribution of Mg, Ti, Cl, O and Fe.

The SEM images show that the unmilled sample (Figure 4a) has distinct phases, heterogeneous size distribution and irregularly shaped particles. In contrast to this, the 30 h milled sample shows a more homogeneous elemental mixture (Figure 4b); the $TiCl_3$ is evenly distributed throughout the mixture and BSE light/dark regions are less distinct. Impurities such as Fe are an inherent consequence of the ball milling process and this is highlighted by the presence of Fe (light regions) after 30 h of milling (Figure 4b). The improved homogeneity of the compounds after milling provides shorter distances between the reactants LiH and MgB_2 as well as an improved distribution of $TiCl_3$. This is also in good correlation with the results shown in Figure 1, where the reaction with a higher concentration of $TiCl_3$ drastically improves reaction kinetics.

Conclusion

The effect of milling parameters in a planetary ball mill for the LiH-MgB_2 system with $TiCl_3$ dopant has been studied with respect to an energy transfer model of the process to the powders. The relationship between sorption times and energy transfer and the physical properties, crystallite size of MgB_2 and the SSA were determined. From these relationships, it appears that at approximately 20 $kJ.g^{-1}$ there are no further benefits to the system with an increase in energy transfer. This was reflected in results of both the crystallite size and specific surface area (SSA). The minimum crystallite size reached for the energy transfer limit was shown to be about 5 nm and with a maximum SSA of approximately 15 $m^2.g^{-1}$. The model does not account for the effect of filling degree, due to the fixed volume of the milling

vial; however, it was determined that a filling degree of 50 % resulted in the fastest sorption times for both absorption and desorption. Finally, the results demonstrate that the homogeneity of the mixture plays an important role for lowering sorption times.

Acknowledgements

References

[1] A. Zuttel, Hydrogen as a future energy carrier, Weinheim : Wiley-VCH, Weinheim, 2008.

[2] S.-i. Orimo, Y. Nakamori, J.R. Eliseo, A. Züttel, C.M. Jensen, Complex hydrides for hydrogen storage, Chem. Rev., 107 (2007) 4111-4132.

[3] A. Züttel, P. Wenger, S. Rentsch, P. Sudan, P. Mauron, C. Emmenegger, $LiBH_4$ a new hydrogen storage material, J. Power Sources, 118 (2003) 1 – 7.

[4] S.-i. Orimo, Y. Nakamori, G. Kitahara, K. Miwa, N. Ohba, S.-i. Towata, A. Züttel, Dehydriding and rehydriding reactions of $LiBH_4$, J. Alloys Compd., 404 (2005) 427-430.

[5] J.J. Vajo, S.L. Skeith, F. Mertens, Reversible Storage of Hydrogen in Destabilized $LiBH_4$, The Journal of Physical Chemistry B, 109 (2005) 3719-3722.

[6] G. Barkhordarian, T. Klassen, R. Bormann, Composite material storing hydrogen and device for the reversible storage of hydrogen, in: International Patent, 2004.

[7] G. Barkhordarian, T. Klassen, R. Bormann, Kinetic investigation of the effect of milling time on the hydrogen sorption reaction of magnesium catalyzed with different Nb_2O_5 contents, J. Alloys Compd., 407 (2006) 249 – 255.

[8] U. Bösenberg, S. Doppiu, L. Mosegaard, G. Barkhordarian, N. Eigen, A. Borgschulte, T.R. Jensen, Y. Cerenius, O. Gutfleisch, T. Klassen, Hydrogen sorption properties of MgH_2–$LiBH_4$ composites, Acta Mater., 55 (2007) 3951-3958.

[9] M. Dornheim, S. Doppiu, G. Barkhordarian, U. Boesenberg, T. Klassen, O. Gutfleisch, R. Bormann, Hydrogen storage in magnesium-based hydrides and hydride composites, Scripta Mater., 56 (2007) 841 – 846.

[10] J. Jepsen, J.M. Bellosta von Colbe, T. Klassen, M. Dornheim, Economic potential of complex hydrides compared to conventional hydrogen storage systems, Int. J. Hydrogen Energy, 37 (2012) 4204-4214.

[11] S. Budin, I.P. Almanar, S. Kamaruddin, N.C. Maideen, A.H. Zulkifli, Modeling of vial and ball motions for an effective mechanical milling process, J. Mater. Process. Technol., 209 (2009) 4312 – 4319.

[12] A.-L. Chaudhary, D.A. Sheppard, M. Paskevicius, C.J. Webb, E.M. Gray, C.E. Buckley, Mg_2Si Nanoparticle Synthesis for High Pressure Hydrogenation, The Journal of Physical Chemistry C, 118 (2014) 1240-1247.

[13] R. Gosalawit-Utke, C. Milanese, P. Javadian, J. Jepsen, D. Laipple, F. Karmi, J. Puszkiel, T.R. Jensen, A. Marini, T. Klassen, Nanoconfined $2LiBH_4$–MgH_2–$TiCl_3$ in

carbon aerogel scaffold for reversible hydrogen storage, Int. J. Hydrogen Energy, 38 (2013) 3275-3282.

[14] J. Puszkiel, F. Gennari, P.A. Larochette, F. Karimi, C. Pistidda, R. Gosalawit-Utke, J. Jepsen, T.R. Jensen, C. Gundlach, J.B. von Colbe, Sorption behavior of the MgH_2–Mg_2FeH_6 hydride storage system synthesized by mechanical milling followed by sintering, Int. J. Hydrogen Energy, 38 (2013) 14618-14630.

[15] C. Suryanarayana, Mechanical alloying and milling, Prog. Mater Sci., 46 (2001) 1-184.

[16] F. Karimi, P.K. Pranzas, A. Hoell, U. Vainio, E. Welter, V.S. Raghuwanshi, C. Pistidda, M. Dornheim, T. Klassen, A. Schreyer, Structural analysis of calcium reactive hydride composite for solid state hydrogen storage, J. Appl. Crystallogr., 47 (2014) 0-0.

[17] M.P. Pitt, Paskevicius, M., Webb, C. J., Sheppard, D. A., Buckley, C. E., Gray, E. M.,, The synthesis of nanoscopic Ti based alloys and their effects on the MgH_2 system compared with the MgH_2 + $0.01Nb_2O_5$ benchmark, Int. J. Hydrogen Energy, 37 (2012) 4227 – 4237.

[18] P.K. Pranzas, M. Dornheim, U. Bosenberg, J.R.A. Fernandez, G. Goerigk, S.V. Roth, R. Gehrke, A. Schreyer, Small-angle scattering investigations of magnesium hydride used as a hydrogen storage material, J. Appl. Crystallogr., 40 (2007) S383 – S387.

[19] F.A. Santos, A.S. Ramos, C. dos Santos, P.A. Suzuki, D. Rodrigues Júnior, Efficiency Evaluation of ZrB_2 Incorporation in the MgB_2 Matrix Phase Using High-Energy Milling, in: Mater. Sci. Forum, Trans Tech Publ, 2010, pp. 82-87.

[20] N. Burgio, A. Iasonna, M. Magini, S. Martelli, F. Padella, Mechanical alloying of the Fe-Zr system. Correlation between input energy and end products, Il nuovo cimento D, 13 (1991) 459-476.

[21] A. Iasonna, M. Magini, Power measurements during mechanical milling. An experimental way to investigate the energy transfer phenomena, Acta Mater., 44 (1996) 1109-1117.

[22] C. Bonatto Minella, E. Pellicer, E. Rossinyol, F. Karimi, C. Pistidda, S. Garroni, C. Milanese, P. Nolis, M.D. Baró, O. Gutfleisch, Chemical State, Distribution, and Role of Ti-and Nb-Based Additives on the $Ca(BH_4)_2$ System, The Journal of Physical Chemistry C, 117 (2013) 4394-4403.

[23] P.K. Pranzas, M. Dornheim, D. Bellmann, K.F. Aguey-Zinsou, T. Klassen, A. Schreyer, SANS/USANS investigations of nanocrystalline MgH_2 for reversible storage of hydrogen, Physica B-Condensed Matter, 385 (2006) 630 – 632.

[24] R.A. Varin, Czujko, Tomasz., Wronski, Zbigniew S. , Nanomaterials for Solid State Hydrogen Storage, Springer US, Boston, MA, 2009.

[25] J. Chen, N. Kuriyama, Q. Xu, H.T. Takeshita, T. Sakai, Reversible Hydrogen Storage via Titanium-Catalyzed $LiAlH_4$ and Li_3AlH_6, The Journal of Physical Chemistry B, 105 (2001) 11214-11220.

[26] P.K. Pranzas, U. Bösenberg, F. Karimi, M. Münning, O. Metz, C.B. Minella, H.W. Schmitz, F. Beckmann, U. Vainio, D. Zajac, Characterization of Hydrogen Storage Materials and Systems with Photons and Neutrons, Adv. Eng. Mater., 13 (2011) 730-736.